Cognitive network hyperactivation and motor cortex decline correlate with ALS prognosis

Roisin McMackin, Stefan Dukic, Emmet Costello, Marta Pinto-Grau, Lara McManus, Michael Broderick, Rangariroyashe Chipika, Parameswaran M. Iyer, Mark Heverin, Peter Bede, Muthuraman Muthuraman, Niall Pender, Orla Hardiman, Bahman Nasseroleslami

Angaben zur Veröffentlichung / Publication details:

McMackin, Roisin, Stefan Dukic, Emmet Costello, Marta Pinto-Grau, Lara McManus, Michael Broderick, Rangariroyashe Chipika, et al. 2021. "Cognitive network hyperactivation and motor cortex decline correlate with ALS prognosis." *Neurobiology of Aging* 104: 57–70. https://doi.org/10.1016/j.neurobiolaging.2021.03.002.

Neurobiology of Aging 104 (2021) 57–70

Contents lists available at ScienceDirect

Neurobiology of Aging

journal homepage: www.elsevier.com/locate/neuaging.org

Cognitive network hyperactivation and motor cortex decline correlate with ALS prognosis

Roisin McMackin[a], Stefan Dukic[a], Emmet Costello[a], Marta Pinto-Grau[a,b], Lara McManus[a], Michael Broderick[a,c], Rangariroyashe Chipika[a,d], Parameswaran M Iyer[a,e], Mark Heverin[a], Peter Bede[a,d], Muthuraman Muthuraman[f], Niall Pender[a,b,e], Orla Hardiman[a,e,#,*], Bahman Nasseroleslami[a,#]

[a] Academic Unit of Neurology, Trinity College Dublin, the University of Dublin, Dublin 2, Ireland
[b] Department of Neurology, University Medical Centre Utrecht Brain Centre, Utrecht University, Utrecht, The Netherlands
[c] Trinity Centre for Bioengineering, Trinity College Dublin, the University of Dublin, Dublin 2, Ireland
[d] Computational Neuroimaging Group, Trinity College Dublin, the University of Dublin, Dublin 2, Ireland
[e] Beaumont Hospital Dublin, Department of Neurology, Dublin 9, Ireland
[f] Biomedical Statistics and Multimodal Signal Processing Unit, Department of Neurology, Johannes-Gutenberg-University Hospital, Mainz, Germany

ARTICLE INFO

Article history:
Received 9 April 2020
Revised 26 February 2021
Accepted 2 March 2021
Available online 10 March 2021

Keywords:
Electroencephalography
Amyotrophic lateral sclerosis
Hyperexcitability
Cognition
Longitudinal
Network

ABSTRACT

We aimed to quantitatively characterize progressive brain network disruption in Amyotrophic Lateral Sclerosis (ALS) during cognition using the mismatch negativity (MMN), an electrophysiological index of attention switching. We measured the MMN using 128-channel EEG longitudinally (2–5 timepoints) in 60 ALS patients and cross-sectionally in 62 healthy controls. Using dipole fitting and linearly constrained minimum variance beamforming we investigated cortical source activity changes over time. In ALS, the inferior frontal gyri (IFG) show significantly lower baseline activity compared to controls. The right IFG and both superior temporal gyri (STG) become progressively hyperactive longitudinally. By contrast, the left motor and dorsolateral prefrontal cortices are initially hyperactive, declining progressively. Baseline motor hyperactivity correlates with cognitive disinhibition, and lower baseline IFG activities correlate with motor decline rate, while left dorsolateral prefrontal activity predicted cognitive and behavioural impairment. Shorter survival correlates with reduced baseline IFG and STG activity and later STG hyperactivation. Source-resolved EEG facilitates quantitative characterization of symptom-associated and symptom-preceding motor and cognitive-behavioral cortical network decline in ALS.

1. Introduction

Amyotrophic lateral sclerosis (ALS) is a progressive neurodegenerative disease defined by the presence of upper and lower motor neuron degeneration. Disease progression is variable with median survival times ranging from 20 to 48 months (Chio et al., 2009). Imaging (Mazón et al., 2018), electrophysiological (Iyer et al., 2017; Vucic et al., 2008) and histological (Gregory et al., 2019) studies have demonstrated that pathologic processes underlying ALS can begin many years before clinical manifestation. This is likely to be due to a combination of reserve neurons facilitating normal function (Eisen et al., 1993) and compensation from other brain regions (Schoenfeld et al., 2005; Witiuk et al., 2014). This observation points to the requirement for diagnostic biomarkers that can identify such early ALS pathology, ideally prior to the earliest point of clinical presentation. Further, as disease heterogeneity is an important confounding factor in clinical trials of potential

Abbreviations: ALS, Amyotrophic Lateral Sclerosis; AEP, Auditory evoked potential; ALSFRS-R, ALS functional rating scale revised; AUROC, Area Under the Receiver-ship Operating Curve; BBI, Beaumont behavioural inventory; CWIT, Colour Word Interference Test; DLPFC, Dorsolateral prefrontal cortex; EBI, Empirical Bayesian Inference; ECAS, Edinburgh cognitive and behavioural ALS screen; EEG, Electroencephalography; ERP, Event related potential; FTD, Frontotemporal dementia; IFG, Inferior frontal gyrus; L, Left; LCMV, Linearly constrained minimum variance; LORETA, Low resolution electromagnetic tomography; MMN, Mismatch negativity; MRI, Magnetic resonance imaging; M1, Primary motor cortex; PET, Positron emission tomorgraphy; PPC, Posterior parietal cortex; STG, Superior temporal gyrus; TMS, Transcranial magnetic stimulation.

* Corresponding author at: Academic Unit of Neurology, Trinity College Dublin, The University of Dublin, Trinity Biomedical Sciences Institute, 152-160 Pearse Street, Dublin D02 R590, Ireland
E-mail address: hardimao@tcd.ie (O. Hardiman).
Joint Last Authorship.

0197-4580/$ – see front matter
https://doi.org/10.1016/j.neurobiolaging.2021.03.002

therapeutic agents, reliable measures which segregate patients by patterns of disease progression are urgently needed.

Most of the existing studies regarding cortical dysfunction in ALS have focussed on resting, widespread cortical activity and connectivity patterns, such as resting state functional magnetic resonance imaging, electroencephalography (EEG) and magnetoencephalography studies, or have employed motor cortical stimulation/engagement paradigms (such as motor cortex transcranial magnetic stimulation combined with electromyography or EEG during movement tasks) (Bizovičar et al., 2014; Kasahara et al., 2012; Proudfoot et al., 2017; Vucic et al., 2018). However it is now well established that non-motor symptoms are also associated with ALS, including cognitive, behavioral and language impairment [for detailed review see William et al., 2020Huynh et al., 2020], with approximately 50% of ALS patients displaying executive dysfunction (Phukan et al., 2012). Further, such nonmotor pathology is relevant to individual prognoses, with cognitive impairment predicting shorter survival times (Elamin et al., 2011). It is therefore imperative that quantitative measures of function/dysfunction in motor and non-motor cortical networks in ALS are developed for clinical prognostic and diagnostic applications.

While structural magnetic resonance imaging (MRI) can capture both motor and non-motor cortical atrophy (Bede and Hardiman, 2014; Finegan et al., 2020), it is unsuitable for some patients, such as those unable to lie flat in a scanner due to respiratory symptoms (Antonescu et al., 2018). Unlike MRI and other structural imaging methods, functional imaging and electrophysiology can capture both primary network dysfunction and excessive, compensatory network function, providing sensitive measures of early pathology which may precede tissue atrophy. While transcranial magnetic stimulation (TMS) of the motor cortex has provided important measures of early motor cortex hyperexcitability and GABA-ergic interneuron decline in ALS (Vucic et al., 2018), the single and paired pulse protocol used in these studies are unsuitable for investigating such changes in non-motor regions such as cognitive networks or in patients lacking target muscle function (see Supplementary Introduction for more detailed comparison of TMS and EEG for study of non-motor networks in ALS).

EEG is accessible to patients with respiratory symptoms when recorded in seated positions and is relatively cost effective (Lystad and Pollard, 2009). Advances in source localisation of EEG signals, including the development of beamforming methods (such as linearly constrained minimum variance, LCMV (Van Veen et al., 1997)), with greater spatial precision than low resolution electromagnetic tomography, LORETA, (Fontanarosa et al., 2004), and use of boundary or finite element models which describe the head tissue with greater accuracy than previously adopted spherical shell models (Fuchs et al., 2002, 2001), have improved spatial resolution to rival other functional imaging methods. These source localisation methods can use personal MRI scans or general templates (see Supplementary Introduction for a discussion). Furthermore, as source resolved EEG directly captures neuronal dysfunction rather than tissue loss or secondary measures (e.g., blood oxygenation or glucose metabolism), it provides excellent temporal resolution, facilitating examination of spatiotemporal patterns of cortical network activation in relation to task cues.

Numerous electrophysiological measurements have shown utility for the measurement of non-motor network impairment in ALS (Cosi et al., 1984; Dukic et al., 2019; McMackin et al., 2020, 2019b; Raggi et al., 2010). The mismatch negativity (MMN) is a particularly attractive EEG measurement for the study of cognitive impairment in ALS patients as the associated paradigm does not require active physical or cognitive engagement by the patients (Näätänen et al., 2014), who may be limited in these capacities due to disease symptoms (see Supplementary Introduction for further introduction to the MMN). The MMN has been employed as an index to measure auditory and cognitive cortical pathophysiology in a number of psychiatric and neurodegenerative diseases (e.g. schizophrenia (Fulham et al., 2014), Parkinson's disease (Brønnick et al., 2010), multiple sclerosis (Jung et al., 2006)), both to increase understanding of the cortical regions affected by those diseases and in search of diagnostic or prognostic disease biomarkers. It has also been employed in clinical trials as an outcome measure of centrally targeted therapeutics (e.g. NCT01556763, NCT00527020, NCT00527020).

We also recently used the MMN as a tool to identify early changes in cognition in ALS, based on its combination of advantages (McMackin et al., 2019b). Having identified delay in the MMN at sensor level in ALS (Iyer et al., 2017), we performed source analysis to identify the associated dysfunctional sources of the waveform and demonstrated the utility of source-imaged EEG for measuring this disease (McMackin et al., 2019b). In that study, we applied three different source analysis pipelines to harness the individual advantages of LCMV, exact LORETA and dipole fitting methods when investigating dysfunctional sources of MMN. Using dipole fitting, we demonstrated that the inferior frontal gyri (IFG) and left superior temporal gyrus (STG) show significantly reduced activity in ALS. Alterations in IFG activity provided excellent discrimination (area under the receivership operating curve>0.9) between controls and ALS patient with greater susceptibility to cognitive decline (*C9orf72* expansion carriers (Byrne et al., 2012), referred to hereafter as *C9orf72*+, and bulbar onset patients (Schreiber et al., 2005)), demonstrating that source engagement during this paradigm can provide more relevant quantitative measures of ALS-related changes compared to sensor level ERP characteristics. Using LCMV as a beamforming analysis we also established abnormal hyperactivity in the left primary motor (M1), dorsolateral prefrontal (DLPFC) and posterior parietal (PPC) cortices (McMackin et al., 2019b). Use of source-analysis in this study provided a major advantage compared to previous studies on cognitive event-related activity in ALS (Hanagasi et al., 2002; Raggi et al., 2010, 2008). However, ALS is highly heterogeneous in its progression between patients. This cross-sectional analysis could not determine the temporal profile of the identified cortical activity changes with respect to disease progression or determine whether such changes can act as a marker of disease progression. We have, therefore, now performed a longitudinal study of MMN source activity change in ALS and the relationship between these EEG measures and ALS progression to improve our understanding of extra-motor cortical dysfunction in ALS and to investigate their predictive and prognostic utility as biomarkers.

In this study, we have now tracked MMN source activity changes in ALS over time. We sought to determine whether progressive changes occur in cortical sources of neuroelectric activity corresponding to abnormal functional changes at baseline in ALS. We also aimed to investigate the relationship between any progressive changes in network function and survival times and disease progression as measured by functional (ALS functional rating scale-revised, ALSFRS-R (Cedarbaum et al., 1999)) and cognitive-behavioral scores (Edinburgh Cognitive and Behavioral ALS Screen, ECAS (Abrahams et al., 2014), and Beaumont Behavioral Inventory, BBI (Elamin et al., 2017)). Finally, to probe the prognostic utility of these electrophysiological measures and the relevance of nonmotor cortical pathology to ALS prognosis, we have investigated whether baseline cortical activity changes are predictive of ALS symptom progression after one year and whether changes in non-motor function associated network hubs relate to survival times.

2. Materials and methods

2.1. Ethical approval

Ethical approval was obtained from the ethics committee of Beaumont Hospital (REC reference: 13/102) and the St. James's Hospital (REC reference: 2017-02). All participants provided written informed consent before participation. All work was performed in accordance with the Declaration of Helsinki.

2.2. Participants

2.2.1. Recruitment

Patient recruitment was undertaken from the National ALS specialty clinic in Beaumont Hospital. Healthy controls included neurologically normal, age-matched individuals recruited from an existing cohort of population-based controls. A total of 71 ALS patients underwent longitudinal recording while 71 healthy controls underwent a single recording session. Of those who underwent recording, 60 patients (17 female; age mean: 60.56 years, range: 32–81 years, standard deviation: 11.49 years) and 62 controls (42 female; age mean: 60.25 years, range: 36–82 years, standard deviation: 10.70 years) were included in final analyses as data lacking clear auditory evoked potentials (AEPs) were excluded (one participant, who did not report hearing issues, showed no AEP over three separate recordings. Remaining excluded participants took part in two or three recordings, showing AEPs in one recording, but no clear AEP in the other(s), due to similar baseline and poststimulus signal amplitudes. Due to lack of longitudinal data of sufficient quality, they were therefore excluded). Patients and controls were age matched ($p = 0.14$) but not gender matched ($p = 3.00 \times 10^{-5}$, $\chi^2 = 17.42$), however we previously established no significant difference between genders for these measures (McMackin et al., 2019b), and we have included gender as a factor in our statistical analysis. Controls did not undergo longitudinal assessment (primarily driven by recruitment difficulty due to hesitation to enrol in longitudinal studies). Significant individual test-retest stability has, however, been previously demonstrated for the MMN (Pekkonen et al., 1995), supporting the stability of measures in controls as baseline.

Patient participants were informed at recruitment that the study was longitudinal (up to five sessions, T1-T5, approximately every four to six months), but that participants were not required to commit to all follow up sessions in order to take part, as high dropout was expected by session four and five (>1 year after baseline recording) due to disease progression. Participant drop out was due to disease progression (resulting in inability to attend the hospital and/or sit upright, relaxed and still due to motor disability).

2.2.2. Inclusion criteria

All participants were over 18 years of age and able to give informed written or verbal (in the presence of two witnesses) consent. Patients were diagnosed with Possible, Probable or Definite ALS in accordance with the El Escorial Revised Diagnostic Criteria (Ludolph et al., 2015).

2.2.3. Exclusion criteria

Exclusion criteria included multiple sclerosis, stroke, seizure disorders, brain tumors, psychological and structural brain diseases, and other relevant neuromuscular comorbidities were excluded.

2.3. Experimental paradigm

The experimental paradigm and data processing pipeline is illustrated (simplified) in Fig. 1. The experimental paradigm is the same as the implementation in our previous cross-sectional studies (Iyer et al., 2017; McMackin et al., 2019b), which is briefly described as follows. Subjects were seated in a chair and asked to relax and watch a silent, black and white film (The Artist, Warner Bros.) while auditory tones were played through headphones (HD650, Sennheiser, Wedemark, Germany). Presentation of a film during recording is part of standard MMN recording protocol (Bonetti et al., 2018; Lonka et al., 2013; Schirmer and Escoffier, 2010) to avoid eye-movements and to prevent participants attending to the tones and performing unrequested mental tasks. As the film is played independently of auditory stimulus presentation and not time locked to any aspect of the task, any cortical activity induced by the film is removed from the ERP via averaging across trials. Participants were instructed to minimize their eye movements, ignore the auditory tones and relax during the EEG acquisition. Standard (720 Hz) and deviant (800 Hz) auditory stimuli were generated by Presentation® (NeuroBehavioral Systems, Inc., Berkeley, CA, USA), such that deviant tones had a higher pitch (i.e., a frequency mismatch). All tones had a duration of 150ms and inter-stimulus-interval of 833ms. Tones were mostly of fixed amplitude (i.e., loudness), set to 50% of desktop output to the headphones (except for a few participants who considered the tones as loud, where this level was reduced). All tones were of fixed amplitude and duration within individuals. Deviant tones were delivered at random amongst standard tones, constituting about 10% of stimuli, with a minimum of 2 standard tones played between each deviant tone. Following a briefing with the participant of what the session involves and informed consenting, the recording session started, which lasted for about 1 hour and 15 minutes (from beginning of equipment setup to end of the paradigm). This included 30 minutes for head measurement, external electrode placement, cap fitting, application of gel and placement of electrodes, 10 minutes for checking and maximisation of recording quality based on online recording and electrode impedance values (to be <25 uV or >-25 uV), 5 minutes for auditory stimulus check, silent film setup and explanation of the task to the participant, 30 minutes for the auditory oddball paradigm.

2.4. Data acquisition

2.4.1. EEG

EEG recordings were conducted in dedicated laboratories in the University of Dublin and St. James's Hospital, Dublin using a BioSemi® ActiveTwo system with 128 active sintered Ag-AgCl electrodes and headcaps (BioSemi B.V., Amsterdam, The Netherlands). EEG data were filtered online over the range 0–134 Hz and digitized at 512 Hz.

2.4.2. ALS functional rating scale revised (ALSFRS-R)

Longitudinal ALSFRS-R data (at least two data points, collected at least 6 months apart) were collected at the National ALS specialty clinic in Beaumont Hospital. These data were collected in a clinical setting and therefore were only collected for those patients who attended the clinic with frequency and timing which sufficiently overlapped with the patient's participation in this study (see results Section 3.1.1).

2.4.3. Cognitive and behavioral tests

Longitudinal Edinburgh Cognitive and Behavioral ALS Screen (ECAS) (Abrahams et al., 2014), Beaumont Behavioral Inventory (BBI) (Elamin et al., 2017) and the Delis-Kaplan Executive Function

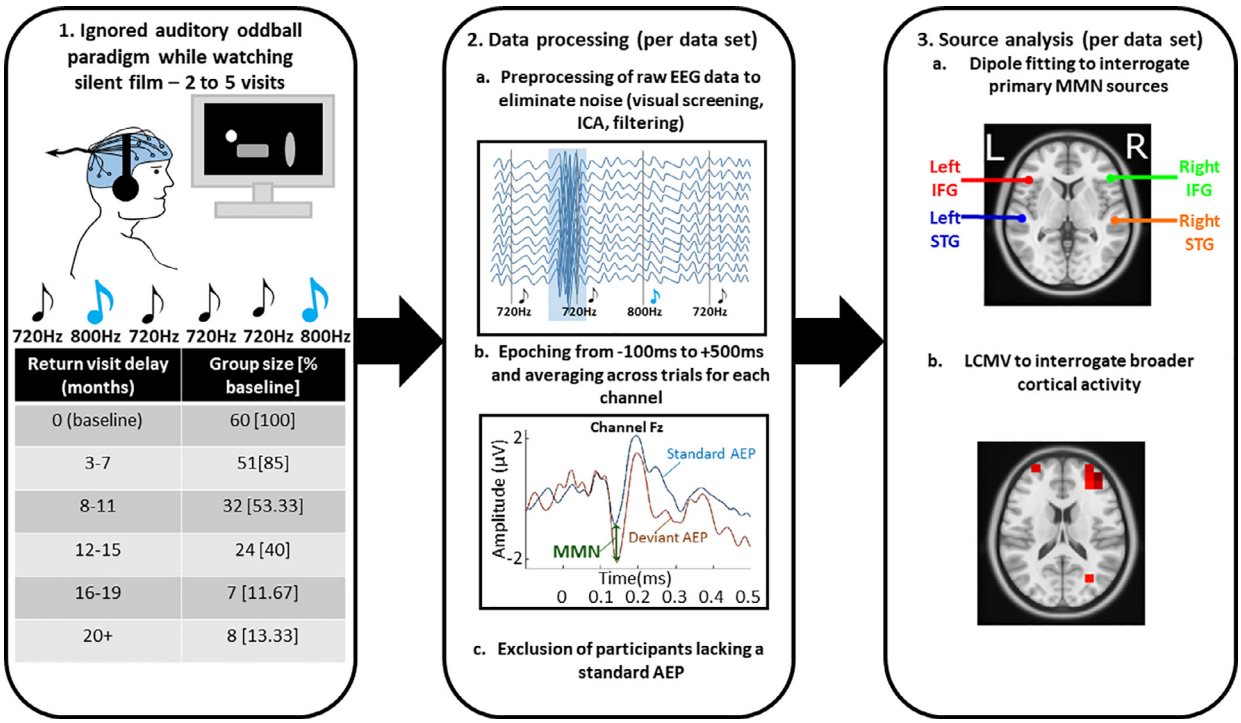

Fig. 1. Illustration of data collection and processing pipeline for each dataset. Frequencies cited refer to the pitch of tones delivered (720 Hz – Standard tone, 800 Hz – Deviant tone). AEP, Auditory evoked potential; MMN, Mismatch negativity; LCMV, Linearly constrained minimum variance; IFG, Inferior frontal gyrus; STG, Superior temporal gyrus; L, Left; R, Right.

System Colour Word Interference Test (CWIT) (Delis et al., 2001) data were also collected as part of a concurrent psychological research study for some participants, who took part in both studies at overlapping time periods (see results section 3.1.1). Versions A, B and C of the ECAS were used for longitudinal cognitive and behavioral screening to avoid practice effects (Crockford et al., 2018).

2.4.4. Survival

Survival was calculated for deceased patients as the number of months between symptom onset and death.

2.5. Data analysis

2.5.1. EEG signal processing

All signal processing and source analysis procedures were identical to that of our cross-sectional study (McMackin et al., 2019b), which are explained as follows. Data were pre-processed using custom MATLAB (R2014a and R2016a, Mathworks Inc., Natick, MA, USA) scripts and the EEGLAB (Delorme and Makeig, 2004) and ADJUST (Mognon et al., 2011) toolboxes. Data were high- and low-pass filtered at cut-off frequencies of 0.3 Hz (dual-pass 5th order Butterworth filter) and 35 Hz (dual-pass 117th order equiripple finite impulse response filter), respectively. Episodes of heavily contaminated signal recordings were identified and removed by visual inspection. Remaining data were epoched to include 100ms prestimulus to 500 ms poststimulus. Independent component analysis (ICA) was then employed to remove stereotyped artefacts (e.g., eye blinks, horizontal eye movements) via decision rules given by ADJUST. Presence of standard tone AEPs was the criterion for inclusion in further analysis. The common-average referenced EEG epochs were then averaged separately for standard and deviant trials to obtain the standard and deviant AEPs, as well as their difference (MMN). The AEPs were baseline-adjusted for analysis.

The number of standard trials was matched to that of deviant trials by random selection for source analysis to avoid bias in LCMV localisation due to differences in the signal to noise ratio (Van Veen et al., 1997). Standard trials were chosen at random, rather than those immediately preceding deviant trials, as some deviant trials were preceded by a standard trial which was eliminated during visual inspection for noise (and therefore would have to be discarded also in the matching process, further reducing signal to noise ratio), and to maintain consistency with existing MMN literature, wherein standard trials are averaged irrespective of their occurrence relative to deviant trials (Garrido et al., 2009). Mean number of included artefact-free standard/deviant trials for controls was 1230/144 and for patients was 1274/145 at T1, 1230/141 at T2, 1182/136 at T3, 1195/136 at T4 and 1137/131 at T5. Therefore, following matching of standard trial numbers (e.g., approximately 140 trials) clear individual AEPs were still obtained from trial means, in alignment with trial numbers of other auditory EEG studies (De Beer et al., 1996; Ethridge et al., 2016; Kaneshiro et al., 2020).

2.5.2. Source analysis

Source analyses were performed using the FieldTrip Toolbox (Oostenveld et al., 2011) and custom scripts in MATLAB (R2016a, Mathworks Inc., Natick, MA, USA). Channels with continuously noisy data were excluded (controls mean [range]: 1.56 [1–7], patients mean [range]: T1: 1.15 [0–5], T2: 1.38 [1–7], T3: 1.29 [1–4], T4: 1.23 [1–3], T5: 1.5 [1–4]) and modeled by spline interpolation of surrounding channels.

Brain, skull, and scalp tissues were modelled using boundary element models. Personal models were generated for 45 patients, using T1-weighted images from MRI. This MRI data were acquired on a 3 Tesla Philips Achieva MRI platform with a maximum gradient strength of 80mT/m using an 8-channel receive-only head coil. T1-weighted images were obtained using a three-dimensional inversion recovery prepared spoiled gradient recalled echo sequence with a field of view of 256 × 256 × 160 mm, spatial resolution:

1 mm^3, TR/TE: 8.5/3.9ms, TI: 1060ms, flip angle: 8°, SENSE factor: 1.5 (Schuster et al., 2017). These MRI were collected on the same day as baseline EEG recording, at the Centre of Advanced Medical Imaging, St. James' Hospital. A ICBM152-based (Fonov et al., 2011) head model was used for remaining patients and controls who declined to/were unsuitable to undergo MRI. Comparable localization accuracy has been demonstrated for template-based and individualised boundary-element head models (Douw et al., 2018; Fuchs et al., 2002), indicating that personalised MRI scans were not essential for modelling. Further, as a single model was used across timepoints for each individual, observed changes in source activity over time are not driven by change in head tissue modelling. For group level analyses, source position coordinate vectors of personal MRI-based head models were warped to those of the ICBM152-based headodels to ensure matching sources were compared.

As we previously identified that the spatial precision of dipole fitting was best suited to the study of the most consistently reported four sources of the MMN while LCMV identified excessive activity of other cortical sources in ALS with better spatial resolution than exact LORETA (McMackin et al., 2019b) we have again used dipole fitting and LCMV for common and uncommon MMN source analysis respectively in keeping with our previous protocol (the design of which is discussed extensively in detail in (McMackin et al., 2019b)). For data processing times see Supplementary Methods.

Details of the source analysis protocol are as follows:

2.5.2.1. Dipole fitting. Dipole fitting (Scherg and Berg, 1991) was used to generate least-square error models of the contributions of the four major established sources of MMN, namely the bilateral inferior frontal gyri and superior temporal gyri (Jemel et al., 2002; Oades et al., 2006; Oknina et al., 2005). Fixed dipoles were modelled at the centroid coordinates of the bilateral superior temporal gyri and pars triangularis of the inferior frontal gyri (right panel, Fig. 1), as determined from an AAL atlas (Tzourio-Mazoyer et al., 2002). Models were estimated based on the average MMN response (mean{deviant response}-mean{standard response}) for 40 ms surrounding the global field power peak between 105 and 271 ms post-stimulus, the period within which we previously demonstrated MMN to be significant (Iyer et al., 2017). Subsequently, mean power for each dipole was calculated. Residual variance (the percentage of variance in the data not accounted for by the model) was used as a measure of goodness of the model fit. The rationale for using this time frame is based upon our previous findings that these four sources better accounted for the data in this window (i.e., had smaller residual variance) than the longer time window of data 100–300 ms post-stimulus, as used for LCMV. We previously demonstrated that a model generated using the longer 200 ms time window provided the same cross-sectional findings (McMackin et al., 2019b).

2.5.2.2. LCMV. To characterise additional cortical source, LCMV was employed by calculating the brain maps of mean power for the average AEP 100-300 ms after standard and deviant cues. Left dorsolateral prefrontal, posterior parietal and motor cortical (chosen based on our previous (McMackin et al., 2019b) cross-sectional statistical analyses) power values were subsequently calculated as the mean LCMV-determined power value of each hyperactive voxel in the left superior and medial frontal gyri (combined), left superior and inferior parietal lobe and left precuneus (combined) and left precentral gyrus respectively, according to the AAL atlas (Tzourio-Mazoyer et al., 2002). Maps of LCMV-determined cortical activity are given as $10\times\log_{10}$(Deviant Power/Standard Power) to prevent single voxel extrema offsetting plot heat maps. Different localisation methods were used for the seven sources of interest based on our previous findings. Namely, while LCMV detected the same trends of dysfunction in the inferior frontal and superior temporal sources as dipole fitting, the effect was spatially distributed such that no specific voxel showed statistically significant differences in ALS. In contrast, the dipole fitting method provides a single measure of power in the region which provided much greater group discrimination (McMackin et al., 2019b).

2.6. Statistics

2.6.1. Comparison of patient and control power

In order to investigate how ALS patient data varied over time relative to control baseline (for example, to investigate if initially underactive sources become normally active or hyperactive), longitudinal data were grouped for comparison to controls. Due to variable intervals between EEG data collection (due to practical aspects and availability of the participants), patient longitudinal data were grouped according to months since first EEG: 0 months (i.e., T1, n = 60), 3–7 months (n = 51), 8–11 months (n = 32), 12–15 months (n = 24), 16–19 months (n = 7), and 20–57 months (n = 8) for comparison to control data. Each ALS patient had a maximum of one data point per time group.

LCMV: For LCMV, a 10mm grid in the brain volume (including white matter regions) yielding 1726 modeled sources was implemented. In order to compare power between patients within each time group to control values for all voxels throughout brain simultaneously, a 10% False Discovery Rate (Benjamini, 2010) was used as a frequentist method for preliminary screening of significant activity difference, corrected across the 1726 source model voxels. Subsequently, Empirical Bayesian Inference (EBI) (Efron, 2009) was used to find Bayesian posterior probabilities, as well as achieved statistical power and Area Under the Receiver Operating Characteristic Curve (AUROC). AUROC is a measure of how well the test separates patient and control groups (Hajian-Tilaki, 2013) which ranges from 0 to 1, where AUROC values further from 0.5 indicate greater group discrimination.

Dipole fitting: For lower dimensional comparison of dipole power for each of the four modelled dipoles, data from the control and ALS patient groups were compared by Mann-Whitney U-test. A 5% FDR was implemented using the Benjamini and Hochberg (1995) method (Benjamini and Hochberg, 1995) to account and correct for multiple comparisons, following the significance testing at $p < 0.05$. Specifically, this FDR was applied across the six time group power values compared to controls power values across all 4 sources of interest (i.e. correction across 24 p-values).

2.6.2. Models of longitudinal change in source power

To investigate change in power over time within ALS patients, the fixed effect of time since T1 and the random effects of delay from symptom onset, gender and age at baseline were simultaneously investigated for each source by linear mixed effects models with the following Wilkinson-style (Wilkinson and Rogers, 1973) model description formula:

$$Power = Time\ since\ T1 + (1|Delay\ from\ symptom\ onset) + (1|Sex) + (1|Age\ at\ baseline) + (Time\ since\ T1|Patient)$$

Intercept and slope were permitted to vary randomly per patient in all models. Group effect (i.e., patient or control) was not incorporated into this analysis the main purpose is to test for longitudinal changes in patients (not measured in controls). For source activity models of the LPPC, LDLPFC, and LM1, power was calculated from the mean activity of voxels within the region demon-

Table 1
Summary of ALS patient clinical characteristics at baseline

Site of onset (spinal/bulbar/thoracic)	50/9/1
C9orf72 expansion carrier (n)	5
Comorbid FTD diagnosis	3
ALSFRS-R (median [IQR])	37.76 [35.80-41.42]
Months since symptom onset (median [IQR])	21.10 [12.26-40.30]
BBI (median [IQR])	4.23 [1.4-7.15]
ECAS total (median [IQR])	113.26 [105.81-118.76]
ECAS ALS specific (median [IQR])	85.30 [77.26-88.11]
ECAS ALS non-specific (median [IQR])	29.25 [26.75-31.89]

Key: IQR, Interquartile range.
Symptom onset date is determined by patient reported estimate.

strating significant hyper activation in our previous cross-sectional analysis. Power values were normalised for linear mixed modelling by inverse normal transformation (Beasley et al., 2009) as residuals were not normally distributed for IFG and STG models without transformation. The null hypothesis of model residuals being normally distributed was not rejected by Shapiro Wilks tests for each model following normalisation of power values ($p > 0.05$).

Linear regression models with time since T1 as the fixed variable and power at source of interest as the dependent variable were also fitted for each source per individual. Robust estimation was used where 3 or more data points were available. Linear regression modelling facilitated clear illustration of the change in individual source activity over time and allowed for assignment of rate of change values to each individual for correlation analyses. Furthermore, these models allowed for estimation of power values for each individual at common time points relative to baseline despite variation across and within datasets in number of data points and intervals between data points (e.g., power at one year after baseline). Second order models (curves) were calculated for all 7 sources per individual, however no quadratic components were deemed significant by sign rank testing (comparing the coefficient value to zero), so further analyses were based on first order models.

Longitudinal analysis was performed with respect to baseline, rather than with respect to patient reported disease onset (Table 1) or time of diagnosis as timing of symptom onset relative to underlying pathophysiology is highly variable in neurodegenerative disease, patient reported disease onset may or may not represent true first disease symptoms as early symptoms may be missed or unrelated events may attributed to the disease, and ALS diagnosis occurs with substantial variation relative to symptom onset and initial clinical presentation. While baseline referencing has similar limitations, it provides a basis for the alignment of individual participation timelines.

2.6.3. Modeling functional and cognitive-behavioral scores for correlation analysis

As intervals between EEG collection and psychological/motor test score collection varied across individuals, linear regression models (robust estimation method used where 3 or more data points were available) were generated for functional or cognitive-behavioral measures (CWIT color naming, word reading, inhibition and inhibition-switching subscores, ECAS total, ECAS ALS-specific, ECAS ALS-nonspecific, ALSFRS-R and BBI scores) for those individuals where 2 data points collected more than 6 months apart were available. In these models, the functional/cognitive-behavioral measure was the dependent variable and time since baseline EEG was the independent variable. Second order models (curves) were also calculated for all scores, however no quadratic components were deemed significant by sign rank testing (comparing the coefficient value to zero). Therefore, the slope (1st order coordinates) of each linear model was used to quantify the rate of change for each measure per individual. Based on these models, the values of each variable (e.g., motor and cognitive-behavioral test scores) at baseline EEG (T1, i.e., 0 months) and after 12 months were calculated.

2.6.4. Correlations

Spearman's nonparametric rank correlation, which is robust to outliers (de Winter et al., 2016), was used to investigate relationships between source activity changes, and between source activity and psychological/motor test scores. Confidence intervals (95%) of rho values were determined by bootstrapping of the rho statistic using 1000 bootstrap samples of the patient dataset with the required clinical scores. Partial correlation was implemented for investigating relationships to CWIT scores, to account for ALSFRS-R speech score at time of CWIT testing, as performance in this task is affected by speech impairment. Multiple comparison correction across the 7 sources of interest, separately for ALS total score (7 comparisons), ECAS total score (7 comparisons), survival (7 comparisons), CWIT scores (4×7 comparisons) and BBI post MND score (7 comparisons) was implemented using a 5% FDR, implemented using the Benjamini and Hochberg method (Benjamini and Hochberg, 1995).

2.6.5. Participant demographics

The differences between age and gender in the patient and control groups were tested by Mann-Whitney U test and chi-squared proportions test respectively.

3. Results

3.1. Participant demographics

3.1.1. Patient clinical data characteristics

ALSFRS-R data were available for 50 patients (n range: 2–20 data points, mean: 10.66). Cognitive-behavioral data were available for 45 (ECAS, n range: 2–5, mean: 3.48), 19 (BBI, n range: 2–4, mean: 3.1) and 19 (CWIT, n range: 3–4, mean: 3.84, one lacking an inhibition switching subscore) patients. The timespan of this data collection overlapped with that of EEG data collection for all but 5 patients, who had a baseline EEG within 6 months after final ECAS follow-up and had either 3 or 4 ECAS data points each spanning at least 14 months, facilitating reliable modeling. Time in months (median [range]) between baseline EEG and nearest data point collection was 0.53 [0–4.11] for ALSFRS-R, 1.74 [0–6.74] for ECAS, 0.20 [0.03–2.10] for CWIT and 1.59 [0.19–5.36] for BBI. Survival data (median: 49.93 months, interquartile range: 35.73–69.69 months) were available for 38 patients, who were deceased by the time of analysis. Patient clinical characteristics at baseline (EEG T1) are summarized in table 1. Overlap in cohort with those included in our previous cross-sectional analysis (McMackin et al., 2019b) includes 34 patients (including all 5 *C9orf72+* patients and 6 of those of bulbar onset) and 39 controls included in this study.

3.2. Cross-sectional analysis

Baseline cross-sectional analysis in this cohort confirms the presence of previously observed abnormal cognitive and motor cortical function. Subgroup cross-sectional analysis was not repeated due to the high overlap of *C9orf72+* and bulbar-onset patients with our previous publication (McMackin et al., 2019b).

At baseline, both IFG showed significantly reduced power (Fig. 2, left: $p = 0.0157$, right: $p = 0.0022$) compared to controls, as we previously observed (McMackin et al., 2019b). While the left

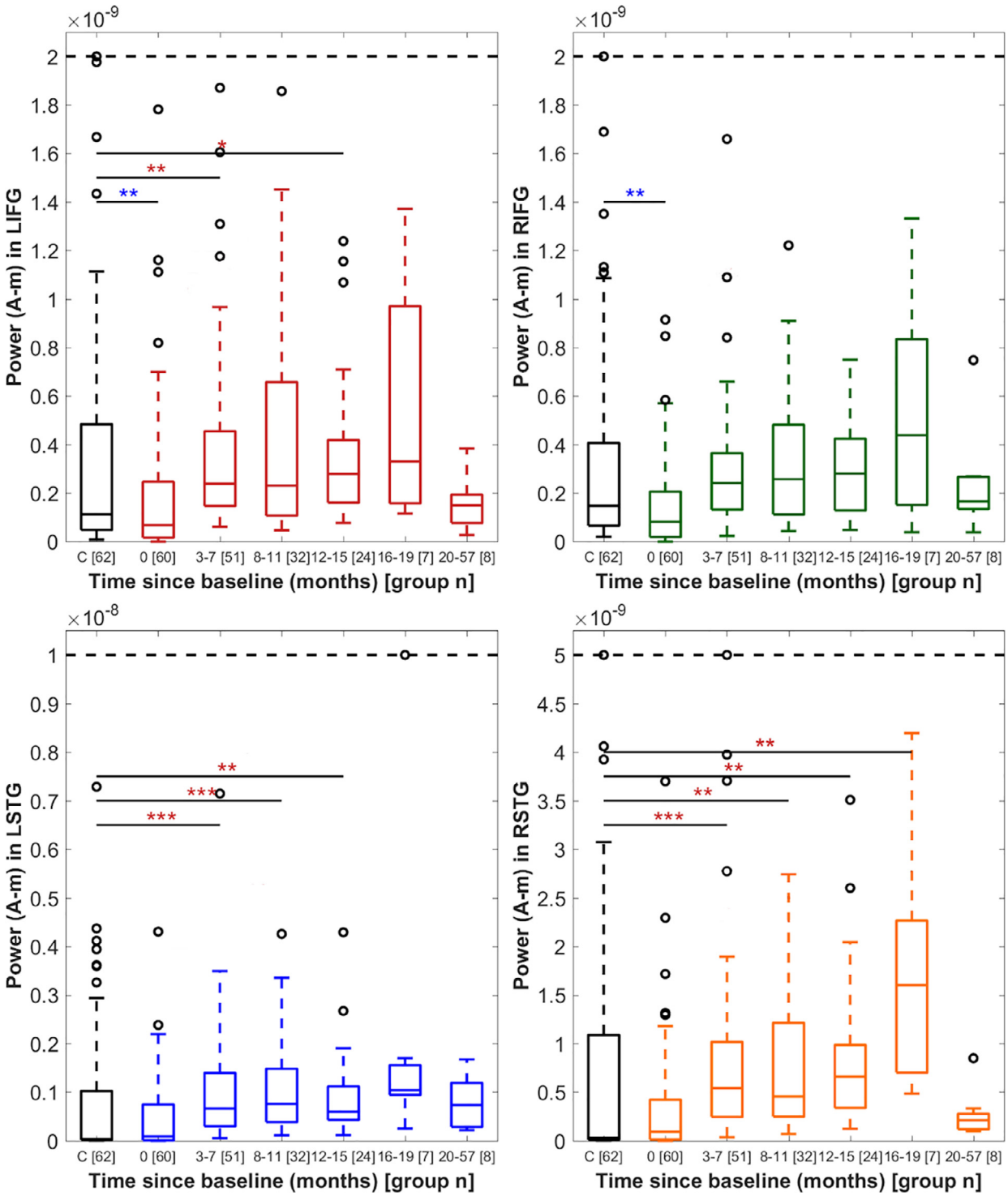

Fig. 2. Comparison of power in each source of MMN, modelled by dipole fitting, between controls and patients at different follow-up times. Significant differences (false discovery rate = 5%) are highlighted by asterisk(s). Red asterisks – Significant increase in patient longitudinal time group power relative to controls. Blue asterisks – Significant decrease in patient longitudinal time group power relative to controls. $^{*}p < 0.05$, $^{**}p < 0.01$, $^{***}p < 0.001$, X axis label shows the time range of the data (in months) in each bin and [group n] values represent datapoints per bin. L/RIFG, Left/right inferior frontal gyrus; L/RSTG, Left/right superior temporal gyrus; C, Controls.

STG showed a trend of decreased activity in line with our previous findings, this difference was not statistically significant (p =0.24). Baseline hyperactivity in left motor, posterior parietal, dorsolateral prefrontal and mid cingulate cortices was again identified in T1 (baseline time point) recordings (Supplementary Fig. 1), consistent with previously findings (McMackin et al., 2019b). Significantly increased activity was also observed within the left medial occipital and right dorsolateral prefrontal cortices. Maximum AUROC was 0.67, in the right middle frontal gyrus.

Table 2
Summary of statistics for significant correlations between EEG measures and clinical characteristics in the ALS patient cohort.

Clinical characteristic	EEG measure	n	Source	Rho	p	Bootstrapping-derived rho confidence interval
Motor						
ALSFRS-R slope	Slope	50	RSTG	−0.40	0.0042	[−0.62,−0.14]
	Power at		LIFG	0.43	0.0022	[0.14,0.61]
	baseline		RIFG	0.47	0.00058	[0.20, 0.67]
ALSFRS-R at baseline			LSTG	−0.37	0.0087	[−0.59, −0.06]
			RSTG	−0.39	0.0058	[−0.61, −0.10]
Survival						
Survival time (months)		38	LIFG	0.49	0.0016	[0.17, 0.69]
			RIFG	0.48	0.0023	[0.21, 0.67]
			LSTG	0.47	0.0032	[0.15, 0.68]
			RSTG	0.48	0.0025	[0.24, 0.68]
Behavioural						
BBI score 1 year after baseline		19	DLPFC	−0.68	0.0017	[−0.84, −0.39]
Cognitive						
ECAS total score 1 year after baseline		46	DLPFC	−0.41	0.0056	[−0.60, −0.12]
CWIT word reading score slope		18	LSTG	0.60	0.0088	[0.13, 0.88]
			RSTG	0.60	0.0086	[0.19, 0.85]
CWIT inhibition switching score slope			LIFG	0.61	0.0098	[0.17, 0.84]
			LSTG	0.73	0.00094	[0.35, 0.92]
			RSTG	0.66	0.0037	[0.27, 0.86]

Key: DLPFC, Left dorsolateral prefrontal cortex; L/R, Left/right; STG, Superior temporal gyrus; IFG, Inferior frontal gyrus; ECAS, Edinburgh Cognitive and Behavioral ALS Screen; BBI, Beaumont Behavioral Inventory, CWIT, Delis-Kaplan Executive Function System Color-Word Interference Test; ALSFRS-R, Revised ALS Functional Rating Scale. Confidence intervals are determined by bootstrapping of the rho statistic using 1000 bootstrap samples of the patient dataset with the required clinical scores (n).

3.3. Longitudinal analysis

Patients took part in a mean of 3.05 sessions (total recording number × number of patients: 2 × 25, 3 × 14, 4 × 14, 5 × 7), with no more than one visit per time point group but potential absence of data in an intermediate time group (for example, data grouped into 0 months, 3–7 and 12–15 months due to delay in return for third recording). Longitudinally, mean residual variance of dipole fitting models was consistent across timepoints and groups (controls: 22%, ALS baseline: 21%, ALS follow up: 3–7 months – 21%, 8–11 months – 25%, 12–15 months - 21%, 16-19 months – 21%, 20–57 months – 18%), demonstrating consistent goodness of fit. At follow up times the left IFG and STG (3–15 months post-baseline) and the right STG (3–19 months post-baseline) showed significantly greater activity than controls, indicating a transition from decreased activity to a state of hyperactivation (Fig. 2). By contrast, the initial hyperactivity observed in the left M1, PPC and DLPFC returned to control levels on inactivity thereafter (i.e., no significant difference from controls). Linear mixed effects modeling demonstrated significant longitudinal decrease in bilateral IFG and STG power and significant longitudinal increase in LDLPFC and LM1 (but not LPPC) power within patients with increasing time from baseline (coefficient *p*-values reported in Fig. 3).

3.4. Correlation with clinical scores

Significant correlations between electrophysiological baseline measures or their rate of change over time and clinical scores are summarized in Table 2. Correlations not deemed significant (corrected $p > 0.05$) are not reported due to the extensive number of correlations performed. All correlations deemed significant by Spearman rank correlation were also deemed significant upon omission of extreme outliers and had a rho value 95% confidence interval derived by bootstrapping that did not cross zero.

3.4.1. Survival

Both IFG and STG baseline activity values correlated with survival, illustrating that those with lower activity at baseline had a poorer outcome.

3.4.2. ALSFRS-R

The mean slope of ALSFRS-R change was 0.57 points per month (range = −1.83 to 0.074, $p = 1.02 \times 10^{-9}$). Significant positive correlations were identified between ALSFRS-R slope and baseline left and right IFG activity. This illustrates that those with lower baseline IFG activity progressed more rapidly (i.e., have a faster rate of ALSFRS-R decline). Further, a significant negative correlation between slope of right STG engagement over time and ALSFRS-R slope was observed (i.e., those whose right STG became more rapidly hyperactive experienced faster ALSFRS-R decline). A significant negative correlation between ALSFRS-R score at baseline recording and STG power at baseline recording was also identified.

3.4.3. Cognitive and behavioral tasks

Slope in word reading score positively correlated with baseline STG activation (i.e. those patients with higher STG engagement at baseline had a faster rate of decline in language function). Rate of change in CWIT inhibition-switching score also correlated with baseline LIFG and bilateral STG activity (i.e., more rapid decline in cognitive flexibility correlates with higher baseline activity in these sources). LDLPFC activity at baseline was negatively correlated with model-interpolated total BBI score (higher score indicates greater behavioral impairment) and ECAS total score (lower score indicates greater cognitive impairment) 12 months later. DLPFC correlations to concurrent BBI and ECAS total scores were not significant with multiple comparison correction.

3.4.4. Correlation between sources

No significant correlations were found between individual model slopes for left M1/DLPFC and those for the left and right

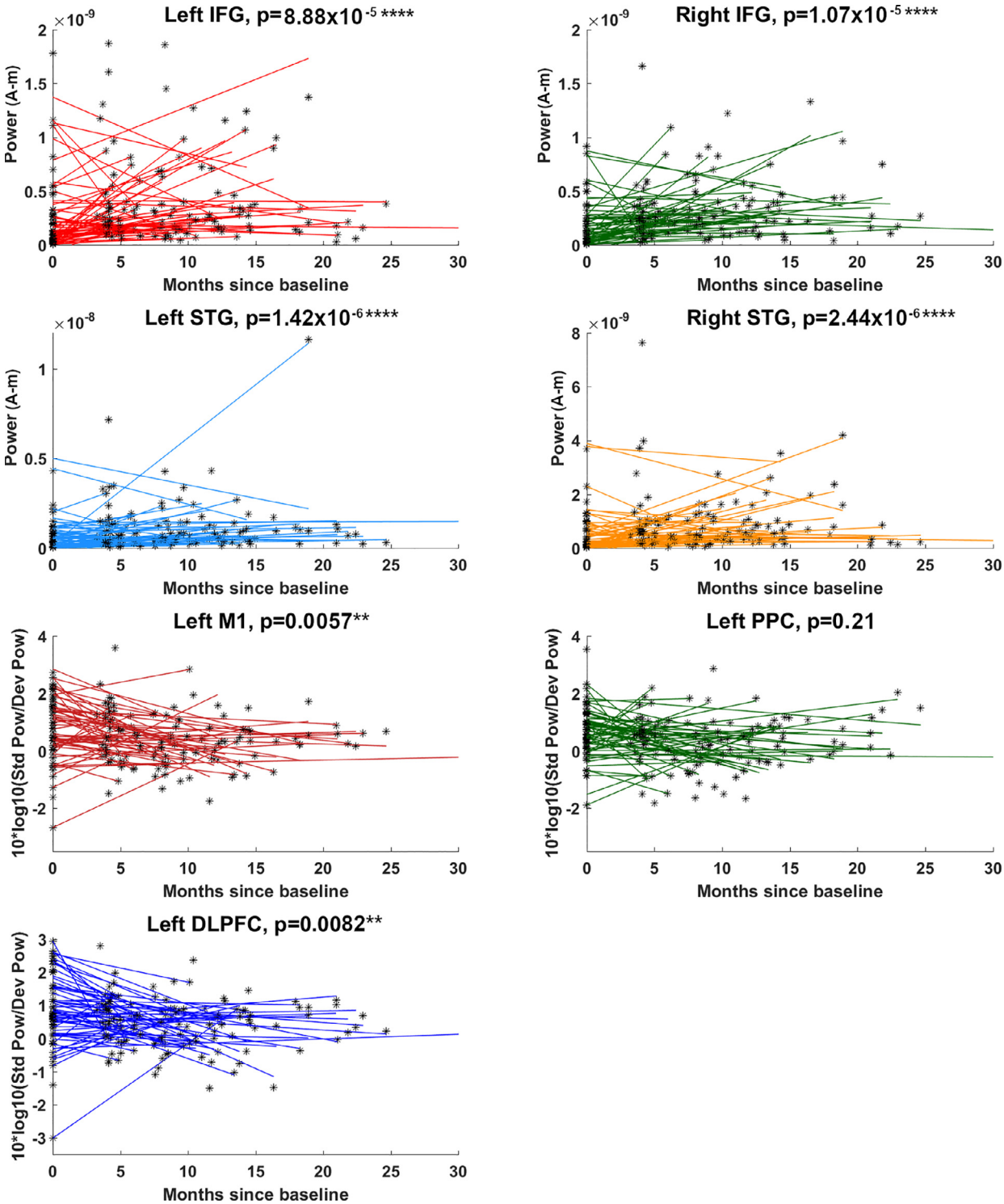

Fig. 3. Modeled source activity change across EEG recording sessions in individual ALS patients. Asterisks indicate individual datapoints while lines represent first order models of data change per participant. P-values listed are the uncorrected values associated with the effect of time since baseline on power in these sources ascertained by linear mixed effects modelling. Title aasterisks denote time since baseline effect coefficient values deemed statistically significant at a 5% FDR. $^{**}p < 0.01$, $^{****}p < 0.0001$ X-axes have been limited to 30 months for clarity (e.g., a single data point at 57 months is not shown). Abbreviations: Power, Power determined by dipole fitting in A-m; Std Pow, Standard power determined by LCMV; Dev Pow, Deviant power determined by LCMV; M1, Primary motor cortex; PPC, Posterior parietal cortex; DLPFC, Dorsolateral prefrontal cortex.

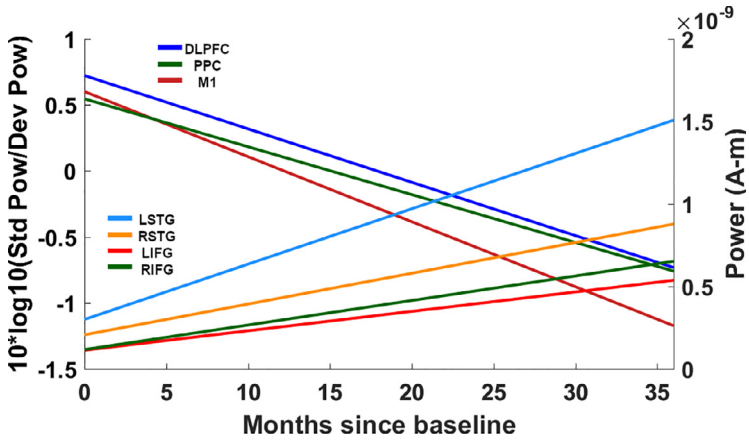

Fig. 4. . Summary of median changes in normal and abnormal MMN sources in ALS patients illustrating that the activity of typical MMN generators increases over time in ALS, whereas the pathologically present activity in nontypical MMN generators declines as disease progresses. Lines represent median slope and intercept of patient models. M1, PPC and DLPFC lines are plotted according to the left-hand y-axis. IFG and STG lines are plotted according to the right-hand y-axis. L/RIFG, Left/right inferior frontal gyrus. L/RSTG, Left/right superior temporal gyrus; DLPFC, Left dorsolateral prefrontal cortex; M1, Left primary motor cortex; PPC, Left posterior parietal cortex.

IFG or STG (n=60 per correlation, 8 correlations performed, all $p >$ 0.39, all absolute rho $<$0.12).

4. Discussion

This study demonstrates that source localized EEG can detect impairments in different regions (nodes) of cortical networks related to ALS progression and may provide useful insight on how the diseases progression takes place. We have identified the emergence of progressive cognitive network hyperactivation in ALS which precedes clinical decline. In addition, we have demonstrated that by directly measuring cortical activity, EEG can detect early pathophysiology that predict current and later cognitive and behavioral symptoms, as well as functional decline measured by ALSFRS-R, and survival.

4.1. Initial suppression and subsequent hyperactivation of the IFG and STG

We previously postulated that decrease in power in IFG and STG sources of MMN reflected an early imbalance between activity in the attentional control networks, with the central executive network being overactive and these nodes suppressed (McMackin et al., 2019b). Our longitudinal data now show that previously observed suppressed nodes become progressively more active to the point of hyperactivation by attention-demanding stimuli with disease progression, as evidenced by significantly greater activity at follow up time points relative to controls as well as relative to baseline. Significant negative correlation between ALSFRS-R score at baseline and STG activation at baseline also highlights that STG suppression is associated with early stages of ALS. These data support the hypothesis that as ALS progresses, initially hyperactive nodes (such as those in the left frontoparietal network) suppress IFG and STG activity. As such early hyperactivation subsequently declines and pathology spreads, the IFG and STG themselves subsequently becoming hyperactive.

Baseline IFG and STG suppression correlates with shorter survival time, with baseline IFG suppression also correlating to more rapid motor decline.

Further, the correlation of greater STG activation at baseline with more rapid deterioration in performance in the CWIT word reading task indicates that hyperactivation of the STG may have pathogenic effects on language functions, known to be affected in some ALS patients (Pinto-Grau et al., 2018). This is in keeping with previous evidence that the STG contributes to language impairment in ALS (for review see Pinto-Grau et al., 2018). A similar correlation was identified between baseline STG and left IFG activity and CWIT inhibition switching score slope. This is likely to reflect the aforementioned relationship to language impairment in the case of the STG. However in the case of left IFG engagement at baseline, as no significant correlations to colour naming or word reading scores were identified, this correlation is likely to reflect a relationship between hyperactivation of the IFG and impaired response inhibition, for which the left IFG has previously been deemed 'critical' (Swick et al., 2008). Taken together, these correlations indicate that those with strong baseline suppression of the IFG and STG experience a fast progressing form of ALS, while those who demonstrated higher IFG and STG activation at baseline may experience a slower progressing form of ALS wherein pathological hyperactivity has time to spread to cognitive and language regions, driving extramotor impairment.

4.2. Initial hyperactivation and progressive inactivity of the motor and dorsolateral prefrontal cortex

Our data show that initial hyperactivity occurs in the primary motor cortex and neighbouring DLPFC, a finding supported by fMRI and other electrical source imaging studies (Dukic et al., 2019; McMackin et al., 2019; Shen et al., 2015). As MMN is a non-motor task, motor cortex hyperactivity may reflect dysregulated inhibitory and/or excitatory input to the upper motor neurons from networks that are activated by the task (McMackin et al., 2019b). Hyperexcitability of upper motor neurons has also been consistently identified by TMS studies, which demonstrate a reduction in the stimulation required to elicit a motor response (Vucic et al., 2018). These studies have attributed motor cortical hyperexcitability to loss of $GABA_A$ inhibitory interneuron function (Vucic et al., 2018). It is likely that this dysfunction characterized in the motor cortex subsequently emerges in the prefrontal and temporal cortex, driving the longitudinal pattern of progressive cortical hyperactivation identified here (Fig. 4).

Given that ALS is characterized by loss of motor neurons, it is to be expected that early motor hyperexcitability wanes with disease progression. This was previously supported by TMS studies which demonstrate elevated motor thresholds or inexcitable motor cortices in some ALS patients (Vucic et al., 2018). Our EEG

work has now definitively demonstrated an initial abnormal activation of the motor cortex which declines longitudinally within individuals which also occurs in the dorsolateral prefrontal cortex. As controls show normal inactivity in the motor cortex during MMN, identification of 'below normal' motor activity is unlikely with this paradigm. The observed changes in ALS patients did not correlate with ALSFRS-R or survival measures.

4.3. Distinct prefrontal pathology relates to cognitive and behavioral impairment in ALS

Left DLPFC activity demonstrated distinct relationships with cognitive and behavioural symptoms. Lower DLPFC activity was associated with greater behavioral impairment, while greater DLPFC activity correlated with greater cognitive impairment. These differing correlations indicate separate cortical pathophysiology underlying ALS with behavioral impairment (ALSbi) and ALS with cognitive impairment (ALSci), which often present clinically independently of one another (Burke et al., 2017). Furthermore, the strengthening of these correlations for future task performance measures, compared to measures of performance at the time of EEG recording, supports our hypothesis that EEG measures of cortical network component dysfunction can predict later symptomatic changes.

4.4. Cortical hyperactivity spread in ALS

The progressive emergence of frontotemporal dementia-like cortical pathophysiology (Cash et al., 2018) is in keeping with the consensus that ALS and FTD are extremes of a single disease spectrum (Strong et al., 2017), with symptoms of one often emerging following a primary diagnosis of the other (Crockford et al., 2018; Hu et al., 2009). The IFG and STG specifically have been identified as predominant areas of grey matter loss in those with frontotemporal dementia and a *C9orf72* expansion (Cash et al., 2018), which is associated with both diseases. Our work shows that early measures of activity in these areas relate to poorer executive and language symptom prognoses, indicating that these changes warrant further investigation as markers of ALS-FTD progression.

4.5. The importance of wider cortical pathology in ALS prognosis

Taken together, our findings demonstrate that symptomatic deterioration in ALS is preceded by changes in indices that capture the spread of pathology through the cortex, rather than indices of motor cortex function alone. While motor cortical dysfunction characterized during this task did not correlate with survival or motor decline, IFG and STG activation at baseline showed highly significant correlations with survival, highlighting the importance of considering pathology beyond the motor cortex in generating effective prognostic biomarkers of ALS. The absence of correlation between motor cortical functional decline and survival, in addition to epidemiological evidence of poorer prognosis in patients with cognitive (Elamin et al., 2011) or behavioral (Chiò et al., 2012) symptoms, and the much slower progression of the upper motor neuron-localised primary lateral sclerosis (Tartaglia et al., 2007), indicates that spread of cortical pathology beyond the motor cortex has greater relevance to ALS prognosis than primary motor cortex decline alone.

We have previously shown that patient subgroups with poorer prognoses and greater susceptibility to cognitive impairment (i.e. *C9orf72*+ and bulbar-onset patients) exhibited greater IFG impairment than the cohort as a whole (McMackin et al., 2019b). Using neuroelectric signal analysis to quantify this more widespread pathology may therefore not only dramatically improve the development of prognostic tools, but also has the potential to provide more personalized and objective measures of the impacts of novel therapeutics on disease progression in clinical trials.

Our study is limited by the availability of psychological task scores, which restricted our exploration of the relationship between cognitive symptoms and source activity. Further, due to small numbers of clinically defined subgroups (e.g., bulbar/thoracic onset) and the prevalence of *C9orf72* expansion-associated ALS in the Irish population, we were limited to performing group-level analysis on ALS patients as a single disease group. Disease heterogeneity was, however examined via modelling and correlation analyses. Additional studies of broader cortical networks, risk gene carriers and larger patient groups, supported by other methods of characterising hyperexcitability (such as single- and paired-pulse TMS-based measures in the case of the motor cortex) are now required to disentangle if patient subcategorization based on spatiotemporal patterns of cortical network malfunction overlap with genetically/clinically defined patient subphenotypes. As this study was not designed or intended to interrogate noncontrasted AEPs, variation in auditory stimulus amplitude was not strictly prohibited to avoid participant discomfort, limiting our ability to use these data to study auditory sensation. Going forward, stimulus amplitude should be recorded for each individual or, if possible, fixed, to facilitate coincident study of early AEP peak characteristics. Finally, the disease progression-related dropout which occurred between return visits is likely to have inflated the proportion of long surviving patients represented in datasets with more return visits. This bias is likely to have affected the sign-rank and Mann-Whitney U test-based group-level longitudinal analysis. Specifically, this bias is likely to have contributed to the lack of statistically significant differences between controls/baseline patient power measurements and patient power measurements 16–19 months or 20–57 months after baseline, despite clear, significant differences at all previous follow up times. This bias should not, however, substantially affect the linear models which were used to determine the rate of change in power in each individual for each source for correlation analysis and which also determined the significant patterns of change longitudinally that were indicated at group level. Should such longitudinal measures be implemented as clinical tools, our modelling indicates that 2–3 recordings is sufficient to capture this change.

Nonetheless, our data demonstrate that the high spatiotemporal resolution of EEG can provide insights into distinct patterns of dysfunction in specific cortical network nodes in ALS. Using this approach, we have identified previously unknown dynamic patterns of cortical dysfunction that relate to ALS progression. EEG with source localization has potential as an inexpensive set of objective prognostic biomarkers and clinical trial outcome measures that are feasible for clinical implementation. Going forward, additional longitudinal investigation is now required to formally quantify the ability of these patterns to predict ALS symptoms as prognostic biomarkers.

Declaration of competing interest

The authors have no actual or potential conflicts of interest.

Data statement

Raw data from this study will be available in anonymized form upon request from qualified investigators subject to the approval by the Data Protection Office (DPO) and Office of Corporate Partnership and Knowledge Exchanges (OCPKE) in Trinity College Dublin, the University of Dublin.

CRediT authorship contribution statement

Roisin McMackin: Conceptualization, Data curation, Formal analysis, Funding acquisition, Investigation, Methodology, Software, Validation, Visualization, Writing – original draft, Writing – review & editing. **Stefan Dukic:** Conceptualization, Data curation, Writing – review & editing. **Emmet Costello:** Conceptualization, Data curation, Writing – review & editing. **Marta Pinto-Grau:** Data curation. **Lara McManus:** Methodology. **Michael Broderick:** Data curation, Software. **Rangariroyashe Chipika:** Data curation. **Parameswaran M Iyer:** Methodology. **Mark Heverin:** Data curation. **Peter Bede:** Data curation, Methodology. **Muthuraman Muthuraman:** Methodology, Writing – review & editing. **Niall Pender:** Methodology, Writing – review & editing. **Orla Hardiman:** Conceptualization, Data curation, Funding acquisition, Investigation, Methodology, Project administration, Resources, Software, Supervision, Writing – review & editing. **Bahman Nasseroleslami:** Conceptualization, Data curation, Funding acquisition, Investigation, Methodology, Project administration, Resources, Software, Supervision, Writing – review & editing.

Acknowledgements

This study was funded by the Irish Research Council [IRC, grant numbers: IRC/EPSPD/2020/108, GOIPG/2017/1014, GOIPD/2015/213], the Health Research Board [HRB, grant numbers: HRA-POR-2013-246, MRCG-2018-02], Science Foundation Ireland [SFI, grant numbers: 16/ERCD/3854] and Research Motor Neurone [grant number: MRCG-2018-02]. Peter Bede and the neuroimaging aspects of the study were supported by the Health Research Board (HRB EIA-2017-019), the Andrew Lydon scholarship, the Iris O'Brien Foundation, the Irish Motor Neurone Disease Association and the Irish Institute of Clinical Neuroscience. The psychology aspects of the study were supported by the Motor Neurone Disease Association [MNDA, grant number: Hardiman/Oct15/879-792]. Muthuraman Muthuraman was supported by the German Research Foundation [grant number: CRC-1193-B05, CRC-TR-128-B05] and Boehringer Ingelheim Funds [grant number: BIF-03]. We thank the Wellcome-HRB Clinical Research Facility at St. James's Hospital in providing a dedicated environment for the conduct of high-quality clinical research. Finally, we would like to thank all the patients, participants and their families who volunteered to take part in this study.

Supplementary materials

Supplementary material associated with this article can be found, in the online version, at doi:10.1016/j.neurobiolaging.2021.03.002.

References

Abrahams, S., Newton, J., Niven, E., Foley, J., Bak, T.H., 2014. Screening for cognition and behaviour changes in ALS. Amyotroph. Lateral Sclerosis Frontotemp. Degen. 15, 9–14. doi:10.3109/21678421.2013.805784.

Antonescu, F., Adam, M., Popa, C., Tuță, S., 2018. A review of cervical spine MRI in ALS patients. J Med. Life 11, 123.

Beasley, T.M., Erickson, S., DB, Allison, 2009. Rank-Based inverse normal transformations are increasingly used, but are they merited? Behav. Genet. 39, 580–595. doi:10.1007/s10519-009-9281-0.

Bede, P., Hardiman, O., 2014. Lessons of ALS imaging: pitfalls and future directions - A critical review. Neuroimage Clin 4, 436–443. doi:10.1016/j.nicl.2014.02.011.

Benjamini, Y., 2010. Discovering the false discovery rate. J. Royal Stat. Soc. Ser. B (Statistical Methodology) 72, 405–416.

Benjamini, Y., Hochberg, Y., 1995. Controlling the false discovery rate: a practical and powerful approach to multiple testing. . Royal Stat. Soc. Ser. B (Methodological) 57, 289–300.

Bizovičar, N., Dreo, J., Koritnik, B., Zidar, J., 2014. Decreased movement-related beta desynchronization and impaired post-movement beta rebound in amyotrophic lateral sclerosis. Clin. Neurophysiol. 125, 1689–1699. doi:10.1016/j.clinph.2013.12.108.

Bonetti, L., Haumann, N.T., Brattico, E., Kliuchko, M., Vuust, P., Särkämö, T., Näätänen, R., 2018. Auditory sensory memory and working memory skills: association between frontal MMN and performance scores. Brain Res. 1700, 86–98. doi:10.1016/j.brainres.2018.06.034.

Brønnick, K.S., Nordby, H., Larsen, J.P., Aarsland, D., 2010. Disturbance of automatic auditory change detection in dementia associated with Parkinson's disease: A mismatch negativity study. Neurobiol. Aging 31, 104–113. doi:10.1016/j.neurobiolaging.2008.02.021.

Burke, T., Pinto-Grau, M., Lonergan, K., Bede, P., O'Sullivan, M., Heverin, M., Vajda, A., McLaughlin, R.L., Pender, N., Hardiman, O., 2017. A Cross-sectional population-based investigation into behavioral change in amyotrophic lateral sclerosis: subphenotypes, staging, cognitive predictors, and survival. Ann. Clin. Transl. Neurol. 4, 305–317. doi:10.1002/acn3.407.

Byrne, S., Elamin, M., Bede, P., Shatunov, A., Walsh, C., Corr, B., Heverin, M., Jordan, N., Kenna, K., Lynch, C., McLaughlin, R., Iyer, P.M., O'Brien, C., Phukan, J., Wynne, B., Bokde, A.L., Bradley, D.G., Pender, N., Al-Chalabi, A., Hardiman, O., 2012. Cognitive and clinical characteristics of patients with amyotrophic lateral sclerosis carrying a C9orf72 repeat expansion: a population-based cohort study. Lancet Neurol. 11, 232–240. doi:10.1016/S1474-4422(12)70014-5.

Cash, D.M., Bocchetta, M., Thomas, D.L., Dick, K.M., van Swieten, J.C., Borroni, B., Galimberti, D., Masellis, M., Tartaglia, M.C., Rowe, J.B., Graff, C., Tagliavini, F., Frisoni, G.B., Laforce Jr., R., Finger, E., de Mendonca, A., Sorbi, S., Rossor, M.N., Ourselin, S., Rohrer, J.D., the Genetic FTD Initiative, GENFI, 2018. Patterns of gray matter atrophy in genetic frontotemporal dementia: results from the GENFI study. Neurobiol. Aging 62, 191–196. doi:10.1016/j.neurobiolaging.2017.10.008.

Cedarbaum, J.M., Stambler, N., Malta, E., Fuller, C., Hilt, D., Thurmond, B., Nakanishi, A., BDNF ALS Study Group (Phase III) Appendix A, 1999. The ALSFRS-R: a revised ALS functional rating scale that incorporates assessments of respiratory function. J. Neurol. Sci. 169, 13–21.

Chiò, A., Ilardi, A., Cammarosano, S., Moglia, C., Montuschi, A., Calvo, A., 2012. Neurobehavioral dysfunction in ALS has a negative effect on outcome and use of PEG and NIV. Neurology 78, 1085–1089. doi:10.1212/WNL.0b013e31824e8f53.

Chio, A., Logroscino, G., Hardiman, O., Swingler, R., Mitchell, D., Beghi, E., Traynor, B.G., Eurals Consortium, 2009. Prognostic factors in ALS: a critical review. Amyotroph. Lateral Scler. 10, 310–323. doi:10.3109/17482960802566824.

Cosi, V., Poloni, M., Mazzini, L., Callieco, R., 1984. Somatosensory evoked potentials in amyotrophic lateral sclerosis. J. Neurol. Neurosurg. Psychiatry 47, 857–861.

Crockford, C., Newton, J., Lonergan, K., Chiwera, T., Booth, T., Chandran, S., Colville, S., Heverin, M., Mays, I., Pal, S., Pender, N., Pinto-Grau, M., Radakovic, R., Shaw, C.E., Stephenson, L., Swingler, R., Vadja, A., Al-Chalabi, A., Hardiman, O., Abrahams, S., 2018. ALS-specific cognitive and behavior changes associated with advancing disease stage in ALS. Neurology 91, e1370–e1380. doi:10.1212/WNL.0000000000006317.

De Beer, N.A., Van Hooff, J.C., Brunia, C.H., Cluitmans, P.J., Korsten, H.H., Beneken, J.E., 1996. Midlatency auditory evoked potentials as indicators of perceptual processing during general anaesthesia. Br. J. Anaesth. 77, 617–624.

Delorme, A., Makeig, S., 2004. EEGLAB: an open source toolbox for analysis of single-trial EEG dynamics including independent component analysis. J. Neurosci. Methods 134, 9–21. doi:10.1016/j.jneumeth.2003.10.009.

Douw, L., Nieboer, D., Stam, C.J., Tewarie, P., Hillebrand, A., 2018. Consistency of magnetoencephalographic functional connectivity and network reconstruction using a template versus native MRI for co-registration. Hum. Brain Mapp. 39, 104–119. doi:10.1002/hbm.23827.

Dukic, S., McMackin, R., Buxo, T., Fasano, A., Chipika, R., Pinto-Grau, M., Costello, E., Schuster, C., Hammond, M., Heverin, M., Coffey, A., Broderick, M., Iyer, P.M., Mohr, K., Gavin, B., Pender, N., Bede, P., Muthuraman, M., Lalor, E., Hardiman, O., Nasseroleslami, B., 2019. Patterned functional network disruption in amyotrophic lateral sclerosis. Hum. Brain Mapp. 40, 4827–4842.

Efron, B., 2009. Empirical Bayes estimates for large-scale prediction problems. J. Am. Stat. Assoc. 104, 1015–1028. doi:10.1198/jasa.2009.tm08523.

Eisen, A., Schulzer, M., MacNeil, M., Pant, B., Mak, E., 1993. Duration of amyotrophic lateral sclerosis is age dependent. Muscle Nerve 16, 27–32. doi:10.1002/mus.880160107.

Elamin, M., Phukan, J., Bede, P., Jordan, N., Byrne, S., Pender, N., Hardiman, O., 2011. Executive dysfunction is a negative prognostic indicator in patients with ALS without dementia. Neurology 76, 1263–1269. doi:10.1212/WNL.0b013e318214359f.

Elamin, M., Pinto-Grau, M., Burke, T., Bede, P., Rooney, J., O'Sullivan, M., Lonergan, K., Kirby, E., Quinlan, E., Breen, N., Vajda, A., Heverin, M., Pender, N., Hardiman, O., 2017. Identifying behavioural changes in ALS: validation of the Beaumont Behavioural Inventory (BBI). Amyotroph. Lateral Scler. Frontotemporal Degen. 18, 68–73.

Ethridge, L.E., White, S.P., Mosconi, M.W., Wang, J., Byerly, M.J., Sweeney, J.A., 2016. Reduced habituation of auditory evoked potentials indicate cortical hyperexcitability in Fragile X Syndrome. Transl. Psychiatry 6, e787. doi:10.1038/tp.2016.48.

Finegan, E., Hi Shing, S.L., Chipika, R.H., McKenna, M.C., Doherty, M.A., Hengeveld, J.C., Vajda, A., Donaghy, C., McLaughlin, R.L., Hutchinson, S., Hardi-

man, O., Bede, P., 2020. Thalamic, hippocampal and basal ganglia pathology in primary lateral sclerosis and amyotrophic lateral sclerosis: Evidence from quantitative imaging data. Data Brief 29. doi:10.1016/j.dib.2020.105115.

Fonov, V., Evans, A.C., Botteron, K., Almli, C.R., McKinstry, R.C., Collins, D.L., Brain Development Cooperative Group, 2011. Unbiased average age-appropriate atlases for pediatric studies. Neuroimage 54, 313–327. doi:10.1016/j.neuroimage.2010.07.033.

Fontanarosa, J.B., Lasky, R.E., Lee, H.C., van Drongelen, W., 2004. Localization of brainstem auditory evoked potentials in primates: a comparison of localization techniques applied to deep brain sources. Brain Topogr. 17, 99–108. doi:10.1007/s10548-004-1007-2.

Fuchs, M., Kastner, J., Wagner, M., Hawes, S., Ebersole, J.S., 2002. A standardized boundary element method volume conductor model. Clin. Neurophysiol. 113, 702–712. doi:10.1016/s1388-2457(02)00030-5.

Fuchs, M., Wagner, M., Kastner, J., 2001. Boundary element method volume conductor models for EEG source reconstruction. Clin. Neurophysiol. 112, 1400–1407. doi:10.1016/S1388-2457(01)00589-2.

Fulham, W.R., Michie, P.T., Ward, P.B., Rasser, P.E., Todd, J., Johnston, P.J., Thompson, P.M., Schall, U., 2014. Mismatch Negativity in Recent-Onset and Chronic Schizophrenia: A Current Source Density Analysis. PLoS One 9. doi:10.1371/journal.pone.0100221.

Garrido, M.I., Kilner, J.M., Stephan, K.E., Friston, K.J., 2009. The mismatch negativity: a review of underlying mechanisms. Clin. Neurophysiol. 120, 453–463. doi:10.1016/j.clinph.2008.11.029.

Gregory, J.M., McDade, K., Bak, T.H., Pal, S., Chandran, S., Smith, C., Abrahams, S., 2019. Executive, language and fluency dysfunction are markers of localised TDP-43 cerebral pathology in non-demented ALS. J. Neurol. Neurosurg. Psychiatry doi:10.1136/jnnp-2019-320807, jnnp-2019-320807.

Hajian-Tilaki, K., 2013. Receiver Operating Characteristic (ROC) Curve Analysis for Medical Diagnostic Test Evaluation. Caspian J. Intern. Med. 4, 627–635.

Hanagasi, H.A., Gurvit, I.H., Ermutlu, N., Kaptanoglu, G., Karamursel, S., Idrisoglu, H.A., Emre, M., Demiralp, T., 2002. Cognitive impairment in amyotrophic lateral sclerosis: evidence from neuropsychological investigation and event-related potentials. Brain Res. Cogn. Brain Res. 14, 234–244.

Hu, W.T., Seelaar, H., Josephs, K.A., Knopman, D.S., Boeve, B.F., Sorenson, E.J., McCluskey, L., Elman, L., Schelhaas, H.J., Parisi, J.E., Kuesters, B., Virginia, M.L., Trojanowski, J.Q., Peterson, R.C., van Swieten, J.C., Grossman, M., 2009. Survival profiles of patients with frontotemporal dementia and motor neuron disease. Arch. Neurol. 66, 1359–1364. doi:10.1001/archneurol.2009.253.

Iyer, P.M., Mohr, K., Broderick, M., Gavin, B., Burke, T., Bede, P., Pinto-Grau, M., Pender, N.P., McLaughlin, R., Vajda, A., Heverin, M., Lalor, E.C., Hardiman, O., Nasseroleslami, B., 2017. Mismatch negativity as an indicator of cognitive subdomain dysfunction in amyotrophic lateral sclerosis. Front. Neurol. 8. doi:10.3389/fneur.2017.00395.

Jemel, B., Achenbach, C., Müller, B.W., Röpcke, B., Oades, R.D., 2002. Mismatch negativity results from bilateral asymmetric dipole sources in the frontal and temporal lobes. Brain Topogr. 15, 13–27.

Jung, J., Morlet, D., Mercier, B., Confavreux, C., Fischer, C., 2006. Mismatch negativity (MMN) in multiple sclerosis: an event-related potentials study in 46 patients. Clin. Neurophysiol. 117, 85–93. doi:10.1016/j.clinph.2005.09.013.

Kaneshiro, S., Hiraumi, H., Sato, H., 2020. Central processing of speech sounds and non-speech sounds with similar spectral distribution: An auditory evoked potential study. Auris Nasus Larynx doi:10.1016/j.anl.2020.02.008.

Kasahara, T., Terasaki, K., Ogawa, Y., Ushiba, J., Aramaki, H., Masakado, Y., 2012. The correlation between motor impairments and event-related desynchronization during motor imagery in ALS patients. BMC Neurosci. 13, 66. doi:10.1186/1471-2202-13-66.

Lonka, E., Relander-Syrjänen, K., Johansson, R., Näätänen, R., Alho, K., Kujala, T., 2013. The mismatch negativity (MMN) brain response to sound frequency changes in adult cochlear implant recipients: a follow-up study. Acta Otolaryngol. 133, 853–857. doi:10.3109/00016489.2013.780293.

Ludolph, A., Drory, V., Hardiman, O., Nakano, I., Ravits, J., Robberecht, W., Shefner, J., WFN Research Group On ALS/MND, 2015. A revision of the El Escorial criteria - 2015. Amyotroph. Lateral. Scler. Frontotemporal Degener. 16, 291–292. doi:10.3109/21678421.2015.1049183.

Lystad, R.P., Pollard, H., 2009. Functional neuroimaging: a brief overview and feasibility for use in chiropractic research. J. Can. Chiropr. Assoc. 53, 59–72.

Mazón, M., Vázquez Costa, J.F., Ten-Esteve, A., Martí-Bonmatí, L., 2018. Imaging biomarkers for the diagnosis and prognosis of neurodegenerative diseases. The Example of amyotrophic lateral sclerosis. Front. Neurosci. 12. doi:10.3389/fnins.2018.00784.

McMackin, R., Bede, P., Pender, N., Hardiman, O., Nasseroleslami, B., 2019a. Neurophysiological markers of network dysfunction in neurodegenerative diseases. Neuroimage Clin. 22, 101706. doi:10.1016/j.nicl.2019.101706.

McMackin, R., Dukic, S., Broderick, M., Iyer, P.M., Pinto-Grau, M., Mohr, K., Chipika, R., Coffey, A., Buxo, T., Schuster, C., Gavin, B., Heverin, M., Bede, P., Pender, N., Lalor, E.C., Muthuraman, M., Hardiman, O., Nasseroleslami, B., 2019b. Dysfunction of attention switching networks in amyotrophic lateral sclerosis. Neuroimage Clin. 22, 101707. doi:10.1016/j.nicl.2019.101707.

McMackin, R., Dukic, S., Costello, E., Pinto-Grau, M., Fasano, A., Buxo, T., Heverin, M., Reilly, R., Muthuraman, M., Pender, N., Hardiman, O., Nasseroleslami, B., 2020. Localisation of Brain networks engaged by the sustained attention to response task provides quantitative markers of executive impairment in amyotrophic lateral sclerosis. Cereb. Cortex 00, 1–13. doi:10.1093/cercor/bhaa076.

Mognon, A., Jovicich, J., Bruzzone, L., Buiatti, M., 2011. ADJUST: An automatic EEG artifact detector based on the joint use of spatial and temporal features. Psychophysiology 48, 229–240. doi:10.1111/j.1469-8986.2010.01061.x.

Näätänen, R., Sussman, E.S., Salisbury, D., Shafer, V.L., 2014. Mismatch negativity (MMN) as an index of cognitive dysfunction. Brain Topogr. 27, 451–466. doi:10.1007/s10548-014-0374-6.

Oades, R.D., Wild-Wall, N., Juran, S.A., Sachsse, J., Oknina, L.B., Röpcke, B., 2006. Auditory change detection in schizophrenia: sources of activity, related neuropsychological function and symptoms in patients with a first episode in adolescence, and patients 14 years after an adolescent illness-onset. BMC Psychiatry 6. doi:10.1186/1471-244X-6-7, 7.

Oknina, L.B., Wild-Wall, N., Oades, R.D., Juran, S.A., Röpcke, B., Pfueller, U., Weisbrod, M., Chan, E., Chen, E.Y.H., 2005. Frontal and temporal sources of mismatch negativity in healthy controls, patients at onset of schizophrenia in adolescence and others at 15 years after onset. Schizophr. Res. 76, 25–41. doi:10.1016/j.schres.2004.10.003.

Oostenveld, R., Fries, P., Maris, E., FieldTrip, Schoffelen J-M., 2011. Open source software for advanced analysis of MEG, EEG, and invasive electrophysiological data. Comput. Intell. Neurosci., 156869 doi:10.1155/2011/156869, 2011.

Pekkonen, E., Rinne, T., Näätänen, R., 1995. Variability and replicability of the mismatch negativity. Electroencephalograp. Clin. Neurophysiol./Evoked Potentials Section 96, 546–554. doi:10.1016/0013-4694(95)00148-R.

Phukan, J., Elamin, M., Bede, P., Jordan, N., Gallagher, L., Byrne, S., Lynch, C., Pender, N., Hardiman, O., 2012. The syndrome of cognitive impairment in amyotrophic lateral sclerosis: a population-based study. J. Neurol. Neurosurg. Psychiatry 83, 102–108. doi:10.1136/jnnp-2011-300188.

Pinto-Grau, M., Hardiman, O., Pender, N., 2018. The Study of Language in the Amyotrophic Lateral Sclerosis - Frontotemporal Spectrum Disorder: a Systematic Review of Findings and New Perspectives. Neuropsychol. Rev. 28, 251–268. doi:10.1007/s11065-018-9375-7.

Proudfoot, M., Rohenkohl, G., Quinn, A., Colclough, G.L., Wuu, J., Talbot, K., Woolrich, M.W., Benatar, M., Nobre, A.C., Turner, M.R., 2017. Altered cortical beta-band oscillations reflect motor system degeneration in amyotrophic lateral sclerosis. Hum. Brain Mapp. 38, 237–254.

Raggi, A., Consonni, M., Iannaccone, S., Perani, D., Zamboni, M., Sferrazza, B., Cappa, S.F., 2008. Auditory event-related potentials in non-demented patients with sporadic amyotrophic lateral sclerosis. Clin. Neurophysiol. 119, 342–350. doi:10.1016/j.clinph.2007.10.010.

Raggi, A., Iannaccone, S., Cappa, S.F., 2010. Event-related brain potentials in amyotrophic lateral sclerosis: A review of the international literature. Amyotroph. Lateral Scler. 11, 16–26. doi:10.3109/17482960902912399.

Scherg, M., Berg, P., 1991. Use of prior knowledge in brain electromagnetic source analysis. Brain Topogr. 4, 143–150.

Schirmer, A., Escoffier, N., 2010. Emotional MMN: Anxiety and heart rate correlate with the ERP signature for auditory change detection. Clin. Neurophysiol. 121, 53–59. doi:10.1016/j.clinph.2009.09.029.

Schoenfeld, M.A., Tempelmann, C., Gaul, C., Kühnel, G.R., Düzel, E., Hopf, J-M., Feistner, H., Zierz, S., Heinze, H.J., Vielhaber, S., 2005. Functional motor compensation in amyotrophic lateral sclerosis. J. Neurol. 252, 944–952. doi:10.1007/s00415-005-0787-y.

Schreiber, H., Gaigalat, T., Wiedemuth-Catrinescu, U., Graf, M., Uttner, I., Muche, R., Ludolph, A.C., 2005. Cognitive function in bulbar- and spinal-onset amyotrophic lateral sclerosis. A longitudinal study in 52 patients. J. Neurol. 252, 772–781. doi:10.1007/s00415-005-0739-6.

Schuster, C., Hardiman, O., Bede, P., 2017. Survival prediction in amyotrophic lateral sclerosis based on MRI measures and clinical characteristics. BMC Neurol. 17, 1–10. doi:10.1186/s12883-017-0854-x.

Shen, D., Cui, L., Cui, B., Fang, J., Li, D., Ma, J., 2015. A systematic review and meta-analysis of the functional MRI Investigation of motor neuron disease. Front. Neurol. 6. doi:10.3389/fneur.2015.00246.

Strong, M.J., Abrahams, S., Goldstein, L.H., Woolley, S., Mclaughlin, P., Snowden, J., Minoshi, E., Roberts-South, A., Benatar, M., Hortobagyi, T., Rosenfeld, J., Silani, V., Ince, P.G., Turner, M.R., 2017. Amyotrophic lateral sclerosis - frontotemporal spectrum disorder (ALS-FTSD): Revised diagnostic criteria. Amyotroph. Lateral Scler. Frontotemporal Degener. 18, 153–174. doi:10.1080/21678421.2016.1267768.

Swick, D., Ashley, V., Turken, A.U., 2008. Left inferior frontal gyrus is critical for response inhibition. BMC Neurosci. 9, 102. doi:10.1186/1471-2202-9-102.

Tartaglia, M.C., Rowe, A., Findlater, K., Orange, J.B., Grace, G., Strong, M.J., 2007. Differentiation between primary lateral sclerosis and amyotrophic lateral sclerosis: examination of symptoms and signs at disease onset and during follow-up. Arch. Neurol. 64, 232–236. doi:10.1001/archneur.64.2.232.

Tzourio-Mazoyer, N., Landeau, B., Papathanassiou, D., Crivello, F., Etard, O., Delcroix, N., Mazoyer, B., Joliot, M., 2002. Automated anatomical labeling of activations in SPM using a macroscopic anatomical parcellation of the MNI MRI single-subject brain. Neuroimage 15, 273–289. doi:10.1006/nimg.2001.0978.

Van Veen, B.D., van Drongelen, W., Yuchtman, M., Suzuki, A., 1997. Localization of brain electrical activity via linearly constrained minimum variance spatial filtering. IEEE Trans. Biomed. Eng. 44, 867–880. doi:10.1109/10.623056.

Vucic, S., van den Bos, M., Menon, P., Howells, J., Dharmadasa, T., Kiernan, M.C., 2018. Utility of threshold tracking transcranial magnetic stimulation in ALS. Clin. Neurophysiol. Pract. 3, 164–172. doi:10.1016/j.cnp.2018.10.002.

Vucic, S., Nicholson, G.A., Kiernan, M.C., 2008. Cortical hyperexcitability may precede the onset of familial amyotrophic lateral sclerosis. Brain 131, 1540–1550. doi:10.1093/brain/awn071.

Wilkinson, G.N., Rogers, C.E., 1973. Symbolic description of factorial models for analysis of variance. J. Royal Stat. Soc. Ser. C (Applied Statistics) 22, 392–399. doi:10.2307/2346786.

William Huynh, Rebekah Ahmed, Colin J. Mahoney, Chilan Nguyen, Sicong Tu, Jashelle Caga, Patricia Loh, Cindy S-Y Lin & Matthew C. Kiernan (2020) The impact of cognitive and behavioral impairment in amyotrophic lateral sclerosis, Expert Review of Neurotherapeutics, 20:3, 281–293, doi:10.1080/14737175.2020.1727740.

de Winter, J.C., Gosling, S.D., Potter, J., 2016. Comparing the Pearson and Spearman correlation coefficients across distributions and sample sizes: a tutorial using simulations and empirical data. Psychol. Methods 21, 273.

Witiuk, K., Fernandez-Ruiz, J., McKee, R., Alahyane, N., Coe, B.C., Melanson, M., Munoz, D.P., 2014. Cognitive deterioration and functional compensation in ALS measured with fMRI using an inhibitory task. J. Neurosci. 34, 14260–14271. doi:10.1523/JNEUROSCI.1111-14.2014.